Cellular and Molecular Life Sciences (2018) 75:4223–4234
https://doi.org/10.1007/s00018-018-2863-3

ORIGINAL ARTICLE

Inhibition of SRC family kinases facilitates anti-CTLA4 immunotherapy in head and neck squamous cell carcinoma

Guang-Tao Yu[1] · Liang Mao[1] · Lei Wu[1] · Wei-Wei Deng[1] · Lin-Lin Bu[1,2] · Jian-Feng Liu[1] · Lei Chen[1] · Lei-Lei Yang[1] · Hao Wu[1] · Wen-Feng Zhang[1,2] · Zhi-Jun Sun[1,2]

Received: 3 January 2018 / Revised: 4 June 2018 / Accepted: 25 June 2018 / Published online: 28 June 2018

Abstract

The immune system plays a critical role in the establishment, development, and progression of head and neck squamous cell carcinoma (HNSCC). As treatment with single-immune checkpoint agent results in a lower response rate in patients, it is important to investigate new strategies to maintain favorable anti-tumor immune response. Herein, the combination immunotherapeutic value of CTLA4 blockade and SFKs inhibition was assessed in transgenic HNSCC mouse model. Our present work showed that tumor growth was not entirely controlled when HNSCC model mice were administered anti-CTLA4 chemotherapeutic treatment. Moreover, it was observed that Src family kinases (SFKs) were hyper-activated and lack of anti-tumor immune responses following anti-CTLA4 chemotherapeutic treatment. We hypothesized that activation of SFKs is a mechanism of anti-CTLA4 immunotherapy resistance. We, therefore, carried out combined drug therapy using anti-CTLA4 mAbs and an SFKs' inhibitor, dasatinib. As expected, dasatinib and anti-CTLA4 synergistically inhibited tumor growth in *Tgfbr1/Pten* 2cKO mice. Furthermore, dasatinib and anti-CTLA4 combined to reduce the number of myeloid-derived suppressor cells and Tregs, increasing the $CD8^+$ T cell-to-Tregs ratio. We also found that combining dasatinib with anti-CTLA4 therapy significantly attenuated the expression of p-$STAT3^{Y705}$ and Ki67 in tumoral environment. These results suggest that combination therapy with SFKs inhibitors may be a useful therapeutic approach to increase the efficacy of anti-CTLA4 immunotherapy in HNSCC.

Keywords CTLA4 · Dasatinib · MDSCs · Tregs · Immunotherapy · HNSCC

Abbreviations

aCTLA4	Anti-CTLA4
CTLA4	Cytotoxic T-lymphocyte-associated antigen 4
Dys	Dysplasia
HNSCC	Head and neck squamous cell carcinoma
HPV	Human papillomavirus
LN	Lymph node
MDSCs	Myeloid-derived suppressor cells
SFKs	Src family kinases
TAMs	Tumor-associated macrophages
TIL	Tumor infiltrate lymphocytes

Guang-Tao Yu and Liang Mao contributed equally.

Electronic supplementary material The online version of this article (https://doi.org/10.1007/s00018-018-2863-3) contains supplementary material, which is available to authorized users.

✉ Wen-Feng Zhang
zhangwf59@whu.edu.cn

✉ Zhi-Jun Sun
sunzj@whu.edu.cn

[1] The State Key Laboratory Breeding Base of Basic Science of Stomatology (Hubei-MOST) and Key Laboratory of Oral Biomedicine, Ministry of Education, School and Hospital of Stomatology, Wuhan University, 237 Luoyu Road, Wuhan 430079, China

[2] Department of Oral Maxillofacial-Head Neck Oncology, School and Hospital of Stomatology, Wuhan University, Wuhan, China

Introduction

Head and neck squamous cell carcinoma (HNSCC) is one of the most common cancers worldwide. Smoking, alcohol exposure and HPV infections are the major risk factors for HNSCC [1]. Although patients can benefit from the advances in surgical techniques, chemotherapy and radiotherapy that have occurred in recent decades, the overall 5-year survival rate of HNSCC has not been improved so far [2].

The immune system plays a critical role in the establishment, development and progression of HNSCC [3]. The exhaustion of tumor-infiltrating T lymphocytes has been reported in many cancers, including HNSCC, and can affect patients' clinical prognosis [4]. In addition, myeloid-derived suppressor cells (MDSCs) and suppressive regulatory T cells (Tregs) have been associated with HNSCC progression [5].

HNSCC is believed to be associated with immunosuppression, characterized by lower counts of tumor-infiltrating T lymphocytes and poor antigen-presenting function [6]. Immune checkpoint receptors are an important group of molecules for immune escape mechanisms in the tumor microenvironment [7]. A series of receptors have been confirmed to be expressed on the surface of dysfunctional T cells, such as cytotoxic T-lymphocyte antigen 4 (CTLA4), programmed death 1 (PD-1), and T-cell immunoglobulin mucin protein 3 (TIM3) [8]. In our previous study, we found that both T cells and certain myeloid cells express CTLA4 in HNSCC. Moreover, blockade of CTLA4 was shown to significantly inhibit tumor growth in the chemopreventive treatment of HNSCC [9].

SRC family kinases (SFKs) are a group of nine intracellularly non-receptor tyrosine kinases, that include c-Src, Fyn, Lyn, and Yes [10]. Activation of SFKs is critical for cancer cells proliferation, migration, invasion, angiogenesis, and metastasis [11]. Therefore, SFKs' inhibitors are promising therapeutics for the treatment of cancer. To date, several SFKs inhibitors, including dasatinib, bosutinib, and saracatinib, have been tested in clinical trials [12, 13].

In this study, we found that effect of inhibiting tumor growth with chemotherapeutic anti-mice CTLA4 is far less than the chemopreventive effect in *Tgfbr1/Pten* 2cKO mice. Moreover, there was no obvious increase in T cells in the tumor microenvironment. Western blotting suggested the increased expression of SFKs after anti-mice CTLA4 chemotherapeutic treatment. In doing so, we hypothesized that the inhibition of SRC family kinases could facilitate chemotherapeutic anti-CTLA4 treatment in *Tgfbr1/Pten* 2cKO mice. Indeed, combining dasatinib and anti-CTLA4 treatment significantly reduced tumor growth and decreased the number of immunosuppressive cells and increased intratumoral of $CD4^+$ and $CD8^+$ T cells in the tumor microenvironment of *Tgfbr1/Pten* 2cKO mice.

Materials and methods

Tgfbr1/Pten 2cKO mouse model

All the mice were maintained in specific pathogen-free condition. All the experimental procedures were approved by the guidelines of the Institutional Animal Care and Use Committee of the Wuhan University (2014LUNSHENZI06 and 2016LUNSHENZI62). Time inducible tissue-specific *Tgfbr1/Pten* 2cKO mice (*K14-Cre*$^{ERtam+/-}$; *Tgfbr1*$^{flox/flox}$; *Pten*$^{flox/flox}$) were maintained and genotyped according to the published protocols [14]. All of the mice were bred on a FVBN/CD1/129/C57 mixed background.

In vivo mouse studies

Chemopreventive treatment: the mice that were assigned to treatment group were treated intraperitoneally (i.p.) with an anti-CTLA4 mAb (9D9; BioXcell: West Lebanon, NH, USA; 10 mg/kg) on days 12, 15, 18, 21, and 24 (after tamoxifen gavage). PBS was used as a negative control for tumorigenesis experiments.

Chemotherapeutic treatment: the treatment group mice were treated i.p. with the anti-CTLA4 mAb (9D9; BioXcell: West Lebanon, NH, USA; 10 mg/kg) on days 26, 33, 40, and 47 (after tamoxifen gavage). The control group was treated with PBS.

Combination treatment: after tamoxifen gavage, all the mice were randomly divided into four groups (n = 5, per group). For the combination treatment group, the anti-CTLA4 mAb were i.p. injected at 10 mg/kg on days 26, 28, 35, 42, 49, and 54 (after tamoxifen gavage) and dasatinib (Selleckchem) was i.p. injected at 10 mg/kg on days 29–33, 36–40, 43–47, and 50–54 (after tamoxifen gavage). For alone anti-CTLA4 mAb treatment group, the mice were treated with the anti-CTLA4 mAb (i.p. at 10 mg/kg) on days 26, 33, 40, 47, and 54 (after tamoxifen gavage). For alone dasatinib treatment group, the mice were injected on days 26–30, 33–37, 40–44, 47–51, and 54 (after tamoxifen gavage). The mice of control group were treated with PBS.

For all of the mice, general inspection and monitoring were carried out every day. The tumor volume was measured using a micrometer caliper and by taking photographs every other day. The endpoint was determined according to a systematic evaluation by the veterinarian. The mice were euthanized at the end of the studies. For subsequent immunostaining or Western blot, the tumor tissues were fixed in formalin overnight or frozen at − 80 °C.

Flow cytometry

Single-cell suspensions were obtained from the tumor of *Tgfbr1/Pten* 2cKO mice. To determine the numbers of MDSCs, the cells were stained with FITC-conjugated anti-CD11b and PE-conjugated anti-Gr-1 (Becton-Dickinson, Mountain View, CA, USA) antibodies. For T-cell analysis, cells were cultured with cell simulation cocktail (eBioscience, San Diego, CA, USA) for 5 h, and then, the cultures were harvested, fixed and permeabilized with fixation and permeabilization buffers (eBioscience, San Diego, CA, USA). The cells were stained with FITC-conjugated

anti-CD4 and anti-CD8 (Becton-Dickinson, Mountain View, CA, USA) antibodies as well as a PE-conjugated anti-IFN-γ (eBioscience, San Diego, CA, USA) antibody. For Tregs analysis, the cells were surface stained with FITC-conjugated anti-CD4 (Becton-Dickinson, Mountain View, CA, USA) and then fixed and permeabilized using the Foxp3/Transcription Factor Staining Buffer (eBioscience, San Diego, CA, USA), and subsequently stained with Percp-cy5.5-conjugated anti-Foxp3 (eBioscience, San Diego, CA, USA). All isotype-matched IgG controls were purchased from eBioscience. Death cells were excluded by staining Fixable Viability Dye eFluor™ 506 (eBioscience, San Diego, CA, USA). The data were analyzed using FlowJo (Tree Star), and gated by the side scatter and forward scatter filters.

Western blot

Tumor tissues from *Tgfbr1/Pten* 2cKO were carefully dissected. Protein concentrations were measured according to a BCA assay (Thermo Scientific, USA) generated standard curve. A total amount of 30 μg protein was denatured and then subjected to 12% SDS-polyacrylamide gel electrophoresis followed by transfer onto polyvinylidene fluoride membranes (Millipore Corporation, Bil-lerica, MA, USA). The membranes was incubated with primary antibodies, washed, and then probed with secondary antibodies. Next, the blots were stained using an enhanced chemiluminescence detection kit (West Pico, Thermo, USA). The following antibodies were used for Western blot: SRC, p-SRC^{Y416}, FAK, and p-FAK$^{Y576/577}$ and STAT3, and p-STAT3^{Y705} (Cell signalling Technology, USA). GAPDH (Cell signalling Technology, USA) was used as a loading control.

Immunofluorescence

Tumor sections were rehydrated in alcohol, washed three times in PBS, retrieved using sodium citrate in a pressure cooker, blocked with 2.5% bovine serum album in PBS buffer for 1 h at 37 °C, and were incubated with primary antibodies (anti-CD4, anti-CD8, and CK-14) overnight at 4 °C, then with the secondary antibodies, and mounted in Vectashield with 4′, 6-diamidino-2-phenylindole (DAPI; Vector Laboratories). Fluorescence images were captured using laser scanning confocal microscope (Olympus, Japan). We used the following antibodies: anti-CD4 (Bio-Rad), anti-CD8 (BD Biosciences), CK-14 (PROGEN, Germany), Alexa 488 anti-Guinea Pig IgG (H + L) (Jackson ImmunoResearch), and Alexa 594 anti-rabbit IgG (Invitrogen, USA). Cell count from ten frames of invasion front was used to calculate counts per square millimeter. The mean value of the ten frames represents the cell count of the section. In addition, the cell count was performed by two individual laboratory technicians.

Immunohistochemistry

First, the 4-μm-thick tumor sections were deparaffinized and rehydrated. Then, for the purpose of antigen retrieval, the sections were boiled in sodium citrate (pH 6.0) or 1-mM ethylene diamine tetra acetic acid (EDTA). Next, the sections were incubated overnight at 4 °C with primary antibodies: p-SRC^{Y416}, p-STAT3Y^{705} (Cell signalling Technology, USA), and Ki-67 (Dako, Denmark). The sections were then incubated with a secondary biotinylated immunoglobulin G antibody solution and an avidin–biotin–peroxidase reagent. Finally, after three times washes with phosphate-buffered saline, the sections were lightly counterstained with Mayer's haematoxylin (Invitrogen, USA). All the sections were scanned by Aperio Image Scope scanner (CA, USA) and quantified by Aperio Quantification software (version 9.1) for nuclear, membrane, or pixel quantification. Then, we selected ten areas of interest in the tumor tissue section and calculated the histoscores as previously described [15]. The mean value of the ten areas represented the histoscores of the section.

Statistical analysis

Data analyses were carried out using Graph Pad Prism version 5.0 for Windows (Graph Pad Software Inc, La Jolla, CA, USA). Differences between two groups were analyzed by a two-tailed Student's *t* test. Differences between three or more group were analyzed by one-way ANOVA followed by the post-Tukey's multiple comparison tests and unpaired *t* test was used to analyze significant difference. Dates are represented as the mean ± SD. *P* values of < 0.05 were considered statistically significant. All results shown in the manuscript are representative of a repeated experiment with similar results.

Results

Anti-CTLA4 treatment is far less effective in tumor growth inhibition when used chemotherapeutically than chemopreventively

Given our previous research finding showing that chemopreventive anti-CTLA4 treatment significantly inhibits tumor growth and reverses the immunosuppression seen in the microenvironment of *Tgfbr1/Pten* 2cKO mice [9], we sought to study the effect of chemotherapeutic anti-CTLA4 for treatment of HNSCC in this model. In the current study, we, therefore, carried out chemopreventive and

chemotherapeutic anti-CTLA4 treatment in *Tgfbr1/Pten* 2cKO mice model. The mice received anti-CTLA4 treatment at 12 days after tamoxifen gavage consistent with our previous study (Fig. 1a) [9]. Chemopreventive anti-CTLA4 treatment effectively inhibited tumor growth (Fig. 1b). In chemotherapeutic treatment experiment, the mice were injected anti-CTLA4 at 26 days after tamoxifen gavage (Fig. 1c). Although chemotherapeutic treatment exhibited some degree of inhibition of tumor growth, compared with control group, the desired strong inhibition was not observed (Fig. 1d), leading us to explore why lead to this situation.

Patterns of intratumoral immune cell populations after therapeutic anti-CTLA4 treatment

Our previous study has indicated that CTLA4 blockade reduced MDSCs as well as Tregs and increased $CD8^+$ T cells in the tumor microenvironment after chemopreventive treatment [9]. In the current study, the number of MDSCs also decreased after chemotherapeutic anti-CTLA4 treatment in *Tgfbr1/Pten* 2cKO mice (Fig. 2a, b). In addition, serial tumor biopsies, which were taken at the endpoint of the treatment, were stained for CD4 and CD8 by immunofluorescence (Fig. 2e; see Additional file 1: Figure S1). We found that chemotherapeutic anti-CTLA4 treatment does not lead to a strong increase in infiltrating $CD4^+$ and $CD8^+$ T cells in the tumor microenvironment (Fig. 2f, g). The number of $CD8^+$ T cells was similarly confirmed by flow cytometry (Fig. 2a). Meanwhile, we analyzed the levels of IFN-γ from $CD8^+$ T cell and $CD4^+FoxP3^+$ Tregs, finding that chemotherapeutic anti-CTLA4 treatment did not significantly increased the levels of IFN-γ from $CD8^+$ T cells (Fig. 2a, c). Furthermore, we assessed the ratio of $CD8^+$ T cell to $CD4^+FoxP3^+$ Tregs in the tumor (Fig. 2d), finding no significant difference between the ratio in the treatment group and control group. These results demonstrated that chemotherapeutic anti-CTLA4 could improve the anti-tumor immunity, but to an insufficient degree to control the tumor.

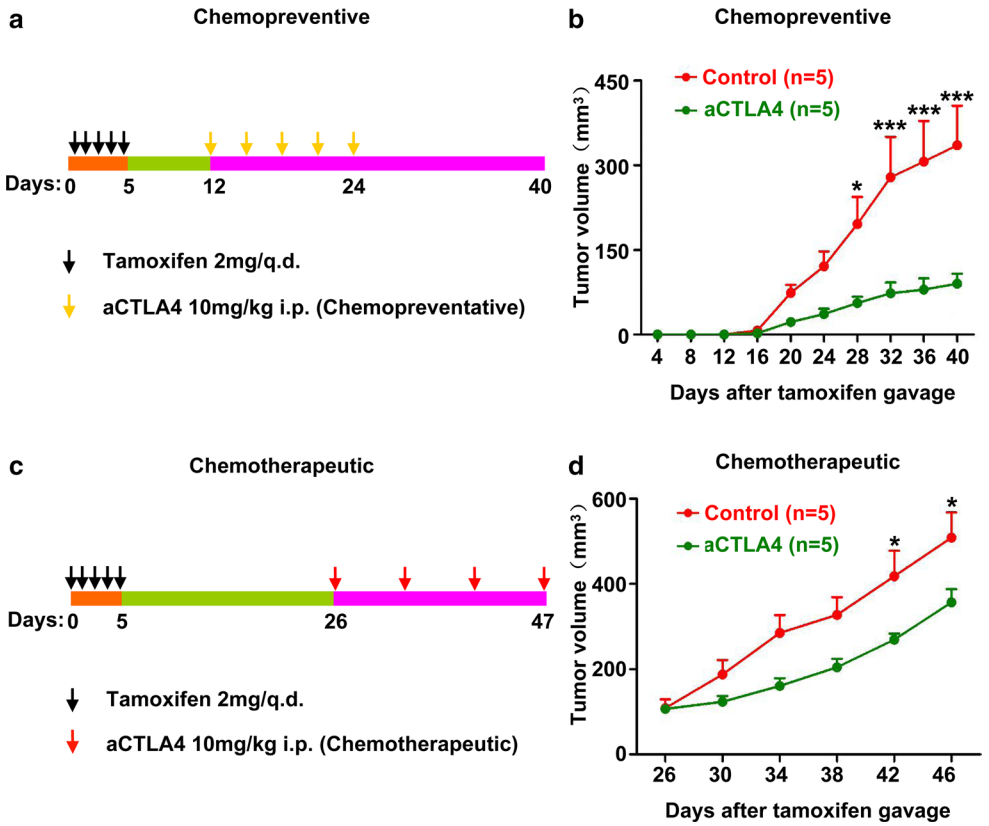

Fig. 1 Therapeutic effects of chemopreventive and chemotherapeutic anti-CTLA4 treatments. **a** Chemopreventive therapy schematic illustration. *Tgfbr1/Pten* 2cKO mice were administered tamoxifen for 5 consecutive days. Anti-mice CTLA4 mAb or PBS were administered i.p. on days 12, 15, 18, 21, and 24 after tamoxifen gavage. Tumor growth was monitored for up to 5 weeks. **b** Tumor growth curves of anti-mice CTLA4 and PBS group. The data are represented as mean ± SD, $n = 5$ (***$p < 0.001$; *$p < 0.05$). **c** Chemotherapeutic treatment schematic illustration. *Tgfbr1/Pten* 2cKO mice were administered tamoxifen for 5 consecutive days. Anti-mice CTLA4 mAb or PBS were administered intraperitoneally on days 26, 33, 40, and 47 after tamoxifen gavage. Tumor growth was monitored for up to 6 weeks. **d** Tumor growth curves of anti-mice CTLA4 and PBS. The data are represented as mean ± SD, $n = 5$ (*$p < 0.05$)

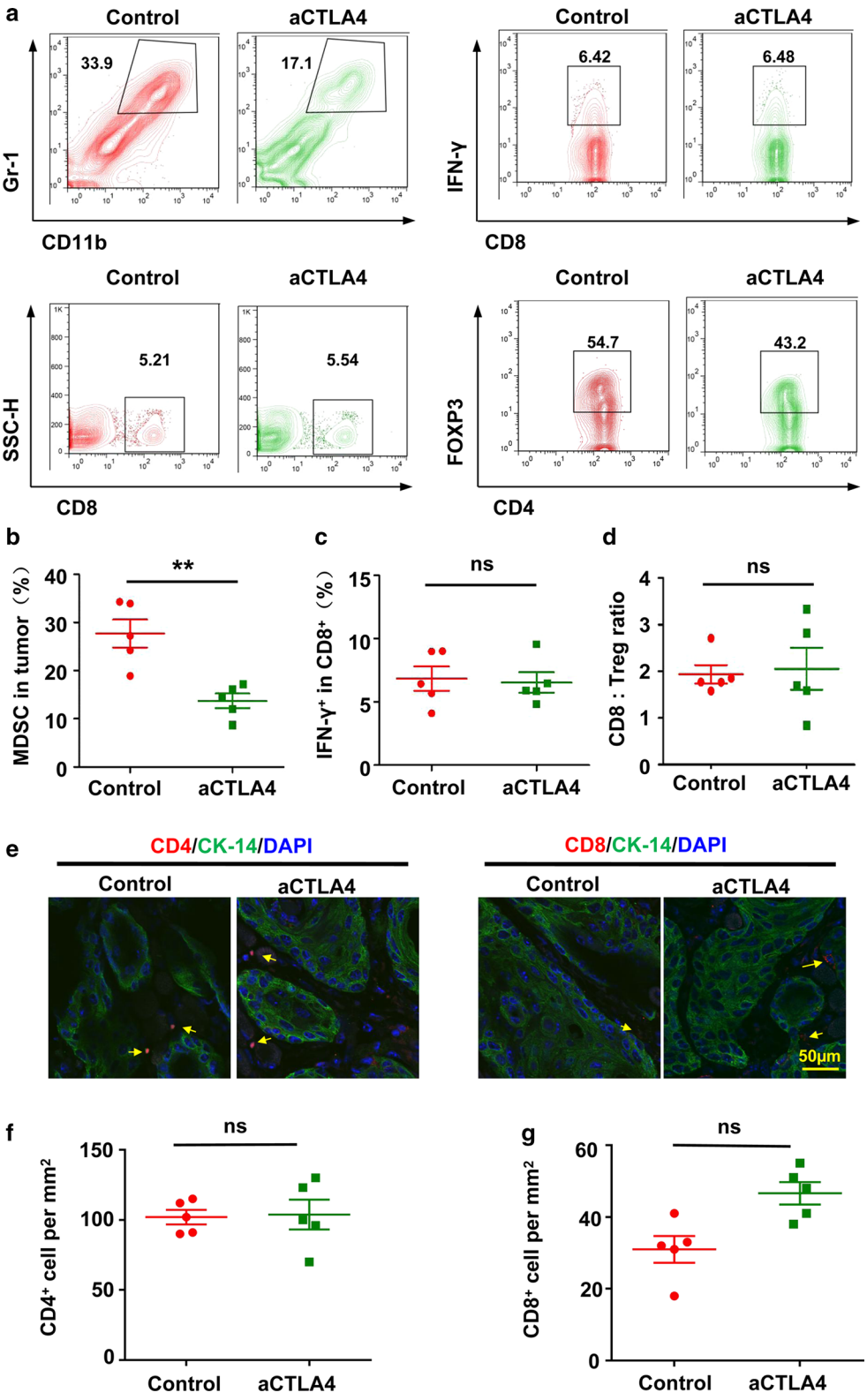

Fig. 2 Influence of chemotherapeutic anti-CTLA4 on the tumor microenvironment. **a** Representative flow cytometry staining of $CD11b^+Gr\text{-}1^+$ MDSCs and $CD8^+$ T cells. Also shown are the number of IFN-γ producing $CD8^+$ T cells and $CD4^+FOXP3^+$ Treg in the tumor. **b** Percentages of $CD11b^+Gr\text{-}1^+$ MDSCs in the gated population from tumor. The data are represented as mean ± SD, $n = 5$ (**$p < 0.01$). **c** Percentages of number of IFN-γ producing $CD8^+$ T cells in the tumor. The data are represented as mean ± SD, $n = 5$ (*ns* not statistically significant). **d** Ratio of $CD8^+$ T cell-to-$CD4^+FOXP3^+$ Treg in the tumor. The data are represented as mean ± SD, $n = 5$ (*ns* not statistically significant). **e** Representative immunofluorescence image for $CD4^+$ and $CD8^+$ T cell in the tumor microenvironment after anti-mice CTLA4 or PBS treatment. Scale bar 50 μm. **f** Quantification of $CD4^+$ cells in tumor from anti-mice CTLA4 or PBS treatment groups. The data are represented as mean ± SD, $n = 5$ (*ns* not statistically significant). **g** Quantification of $CD8^+$ cells in tumor from anti-mice CTLA4 or PBS treatment groups. The data are represented as mean ± SD, $n = 5$ (*ns* not statistically significant)

Therapeutic anti-CTLA4 treatment activated SRC family proteins

SFKs, an intracellularly located group of non-receptor tyrosine kinases, are involved in tumor progression, such as the epithelial-to-mesenchymal transition and cancer stem cells. Using the STRING database, we generated in silico prediction for the protein–protein interactions for SRC and

LYN. Interestingly, both SRC and LYN are the first neighbor protein–protein interaction with CTLA4 (see Additional file 2: Figure S2). Taken together with the literature and data supporting the combined effect of SFKs inhibitor and other chemotherapeutic agent and the bioinformatics evidence for the relationship between SFKs and CTLA4, we tested the phosphorylation level of SFKs after chemopreventive and chemotherapeutic antiCTLA4 treatment. Chemopreventive treatment resulted in decreases in the expression level of p-SRC^{Y416} (Fig. 3a). In contrast, chemotherapeutic treatment promoted the expression of p-SRC^{Y416} (Fig. 3b). Furthermore, after chemotherapeutic anti-mice CTLA4 treatment

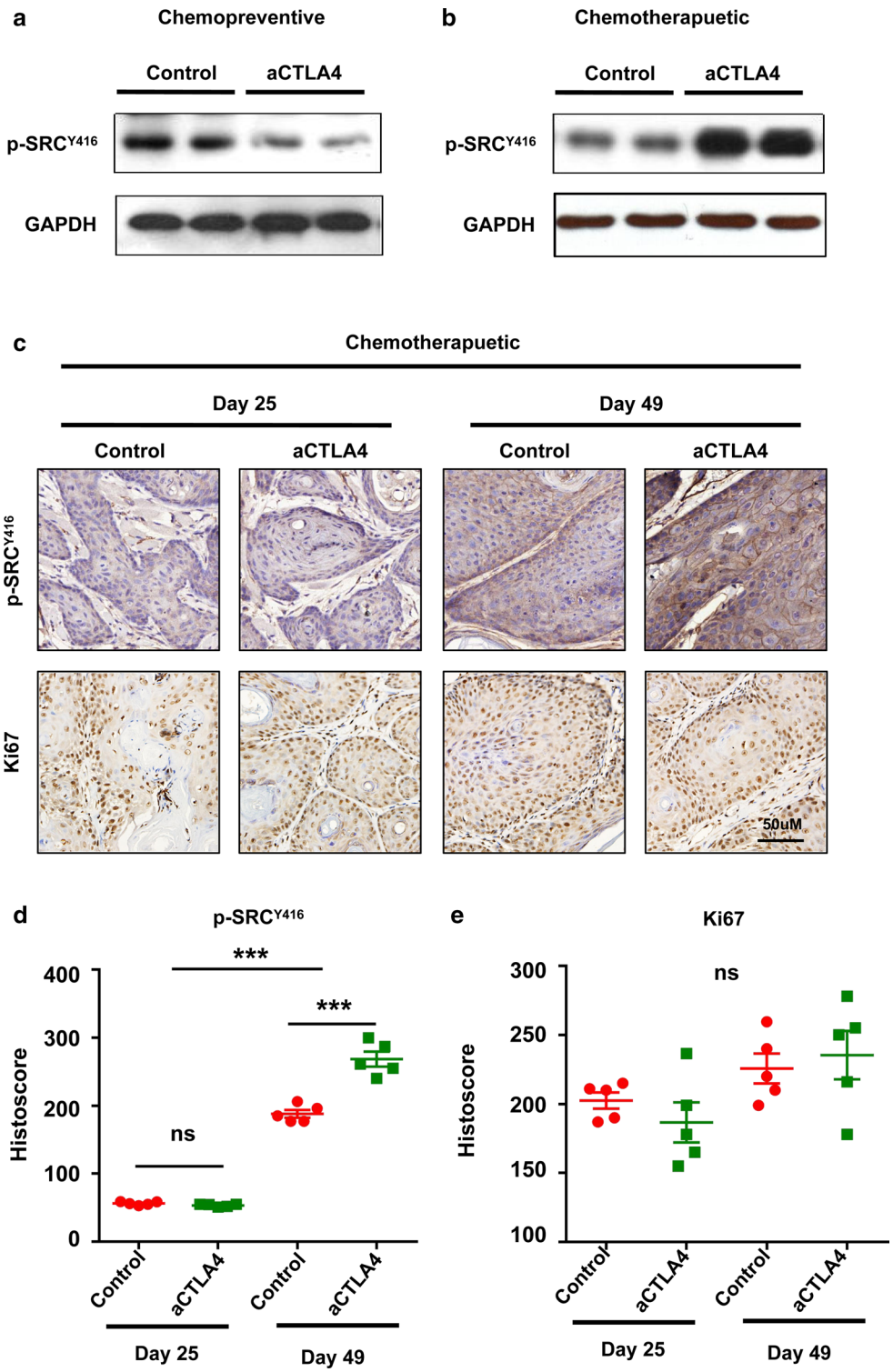

Fig. 3 Difference in SRC family protein levels after chemopreventive and chemotherapeutic anti-mice CTLA4 treatments. **a** Western blot analysis of p-SRC^{Y416} expression in the tumor after chemopreventive anti-CTLA4 treatment. GAPDH was used as the loading control. **b** Western blot analysis p-SRC^{Y416} expression in the tumor after chemotherapeutic anti-CTLA4 treatment. GAPDH was used as the loading control. **c** Representative tumor immunohistochemistry images from the chemotherapeutic treatment or control groups for p-SRC^{Y416} and Ki67 on the day 25 and day 49 after tamoxifen inducing. Scale bar 50 μm. **d** Quantification of p-SRC^{Y416} staining in tumor tissues of anti-mice CTLA4 or PBS treatment groups on the day 25 and day 49 after tamoxifen inducing. The data are represented as mean ± SD, $n = 5$ (***$p < 0.001$; *ns* not statistically significant). **e** Quantification of Ki67 staining in tumor tissues of anti-mice CTLA4 or PBS treatment groups on the day 25 and day 49 after tamoxifen inducing. The data are represented as mean ± SD, $n = 5$ (*ns* not statistically significant)

in the tumor tissue, we found that SFKs expression level was increased, but the Ki67 was not decreased (Fig. 3c–e). We, therefore, speculated that inhibition of SFKs promotes anti-CTLA4 immunotherapy for HNSCC.

Dasatinib has combinatorial activity with anti-CTLA4 in the *Tgfbr1/Pten* 2cKO mouse model

We next assessed the combination of dasatinib and CTLA4 inhibition in our *Tgfbr1/Pten* 2cKO mice. Anti-CTLA4 treatment began on day 26 after tamoxifen gavage. The specific drug delivery strategies are shown in Fig. 4a. While dasatinib and anti-CTLA4 alone exhibited anti-tumor effects in this mouse model, the combination of dasatinib and anti-CTLA4 resulted in significantly greater tumor growth inhibition (Fig. 4b, c). Tumor growth in each mouse in the combination treatment group was strongly inhibited (Fig. 4d). In addition, mice tolerated the combination treatment well, with no apparent weight loss (see Additional file 3: Figure S3).

Combining dasatinib and anti-CTLA4 reduced immunosuppressive cells and increased intratumoral $CD4^+$ and $CD8^+$ T cells in the tumor microenvironment

To study the effects of dasatinib alone, anti-CTLA4 alone or a combination treatment, we compared MDSCs, Tregs, $CD4^+$, and $CD8^+$ T-cell counts in the tumor microenvironment. Using flow cytometry, we detected that the immunosuppressive MDSCs were significantly decreased in each treatment group (Fig. 5a, b). In combination group, there was a notable increase in the number of $CD8^+$ T cells, compared with either treatment alone (Fig. 5a, b).

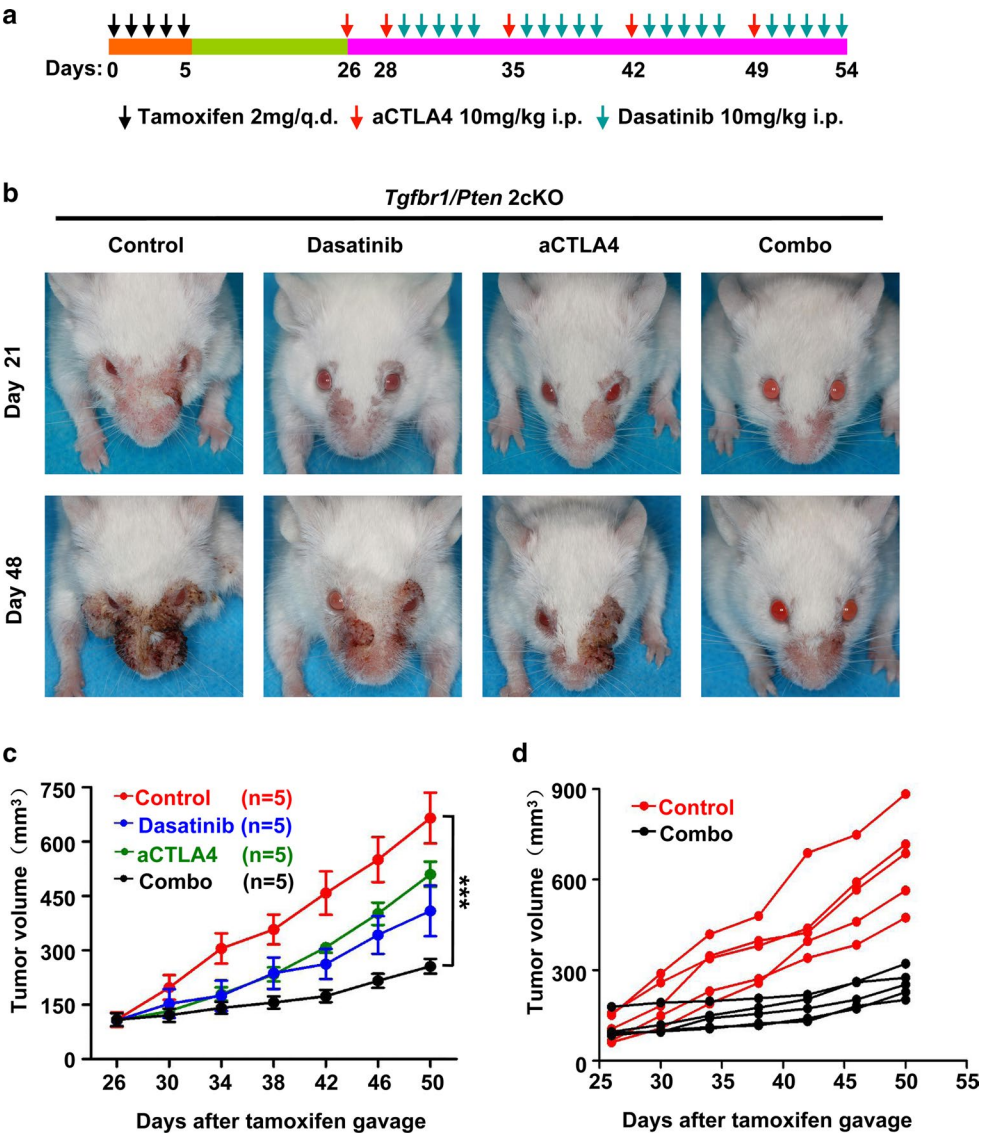

Fig. 4 Combination therapeutic effect of dasatinib and anti-mice CTLA4 mAb in *Tgfbr1/Pten* 2cKO HNSCC mouse model. **a** Schema of treatment. The mice received gavage of tamoxifen for 5 consecutive days. Anti-CTLA4 mAb were administered intraperitoneally on days 26, 28, 35, 42, and 49 after tamoxifen gavage. Dasatinib was administered i.p. on days 29–33, 36–40, 43–47, and 50–54 after tamoxifen gavage. **b** Representative images of a tumor from *Tgfbr1/Pten* 2cKO HNSCC mice treated with PBS, alone anti-mice CTLA4 mAb, alone dasatinib, combining anti-CTLA4 mAb and dasatinib treatment at days 21 and days 48 after tamoxifen gavage. **c** Tumor volume of mice in the four different groups ($n=5$ each group, The data are represented as mean ± SD, $***p<0.001$). **d** Plots represent the tumor volume of individual mice for the control and combination treatment groups

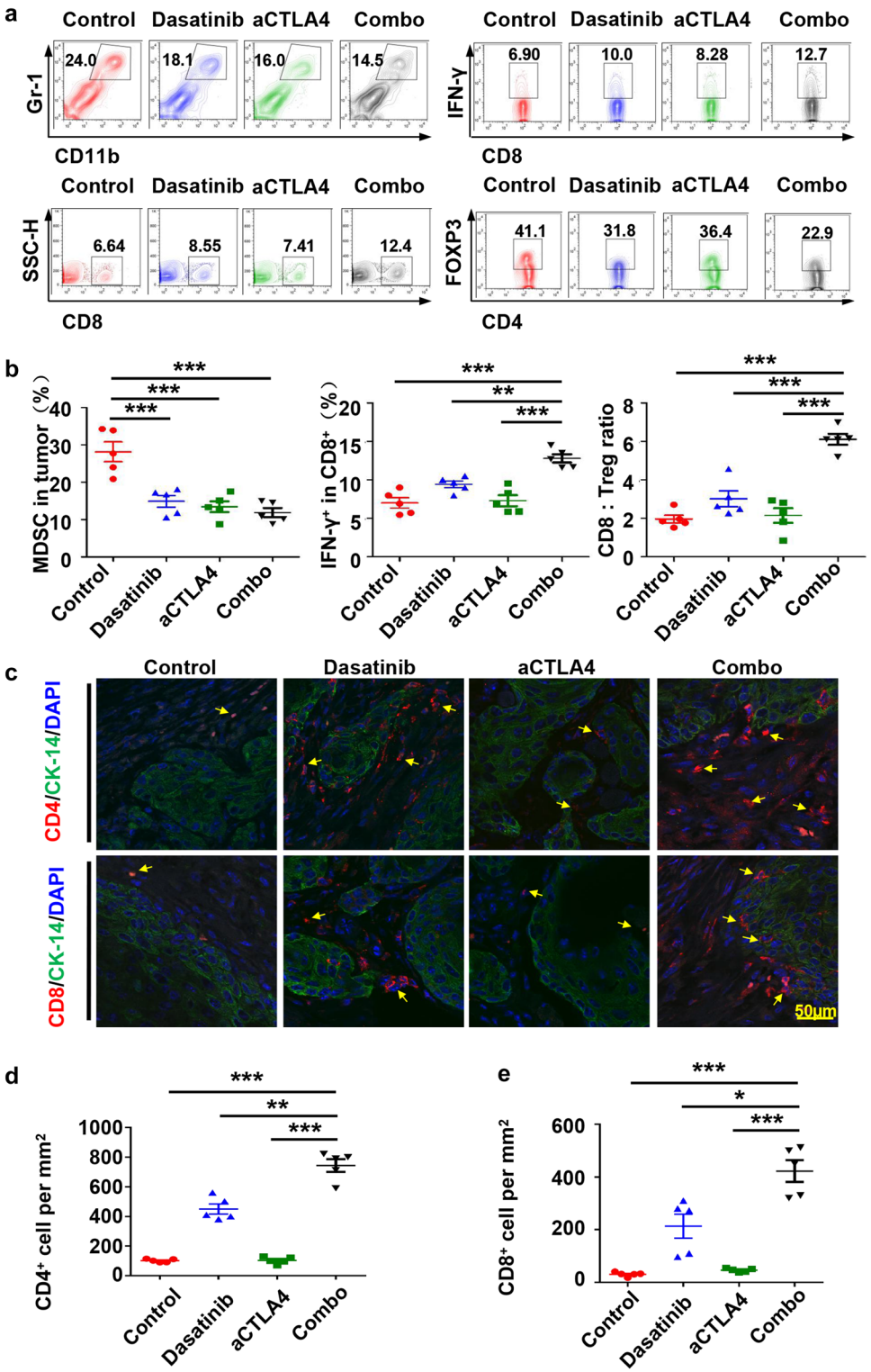

Fig. 5 Patterns of intratumoral immune cell populations after combination therapy with dasatinib and anti-CTLA4 mAb. **a** Single-cell suspensions from tumors were stained for $CD11b^+Gr\text{-}1^+$ MDSCs; $CD8^+$ T cell after single or combination treatment. In addition, the numbers of IFN-γ producing $CD8^+$ T cells and $CD4^+FOXP3^+$ Tregs were determined. **b** The percentages of $CD11b^+Gr\text{-}1^+$ MDSCs in the gated population from tumor (left); the percentages of number of IFN-γ producing $CD8^+$ T cells in the tumor (middle); and the ratio of $CD8^+$ T-cell-to-$CD4^+FOXP3^+$ Tregs in the tumor (right) (the data are represented as mean ± SEM, $n = 5$. $^*p < 0.05$; $^{**}p < 0.01$; $^{***}p < 0.001$). **c** Representative immunofluorescence image of $CD4^+$ and $CD8^+$ T cells in tumor microenvironment after PBS, alone anti-CTLA4 mAb, alone dasatinib, or combination treatment. Scale bar 50 μm. **d** Quantification of $CD4^+$ cells in tumor from PBS, alone anti-CTLA4 mAb, alone dasatinib, or combination treatment groups. The data are represented as mean ± SD, $n = 5$ ($^{**}p < 0.01$; $^{***}p < 0.001$). **e** Quantification of $CD8^+$ cells in tumor from PBS, alone anti-CTLA4 mAb, alone dasatinib, or combination treatment groups. The data are represented as mean ± SD, $n = 5$ ($^*p < 0.05$; $^{***}p < 0.001$)

Meanwhile, the IFN-γ secretion of $CD8^+$ T cells was also enhanced in the combination treatment group (Fig. 5a, b). Another immunosuppressive cell type (Tregs, measured by $Foxp3^+$ and $CD4^+$) were changed less than 1.8-fold for control group, 1.4- and 1.4-fold, respectively, compared with dasatinib treatment group and anti-CTLA4 treatment group (Fig. 5a). Moreover, the ratio of CD8:Tregs has been observably improved in the combination treatment group (Fig. 5b). These data suggested that anti-tumor immunity has been enhanced after combining dasatinib and anti-CTLA4

treatment. Indeed, we observed infiltration of $CD4^+$ and $CD8^+$ T cells in the tumor microenvironment (Fig. 5c–e; see Additional file 4: Figure S4).

The combination of dasatinib and anti-CTLA4 leads to down-regulation of STAT3 phosphorylation and reduced proliferation of tumor cell in this mouse model

We next tested the relative protein expression in each group by western blot. As expected, SFKs signalling protein of p-SRC^{Y416} and p-FAK$^{Y576/577}$ showed notable decrease in the combination treatment group (Fig. 6a). An unexpected finding was pronounced that STAT3 phosphorylation was gradually inhibited by dasatinib alone, anti-CTLA4 alone, or the combination treatment (Fig. 6a). The expression of these proteins was quantified (Fig. 6b), and changes in p-SRC^{Y416} and p-STAT3^{Y706} expression were also assessed via immunohistochemistry (Fig. 6c, d). In addition, we observed synergistic inhibition of tumor proliferation in the combination treatment group (Fig. 6c, d).

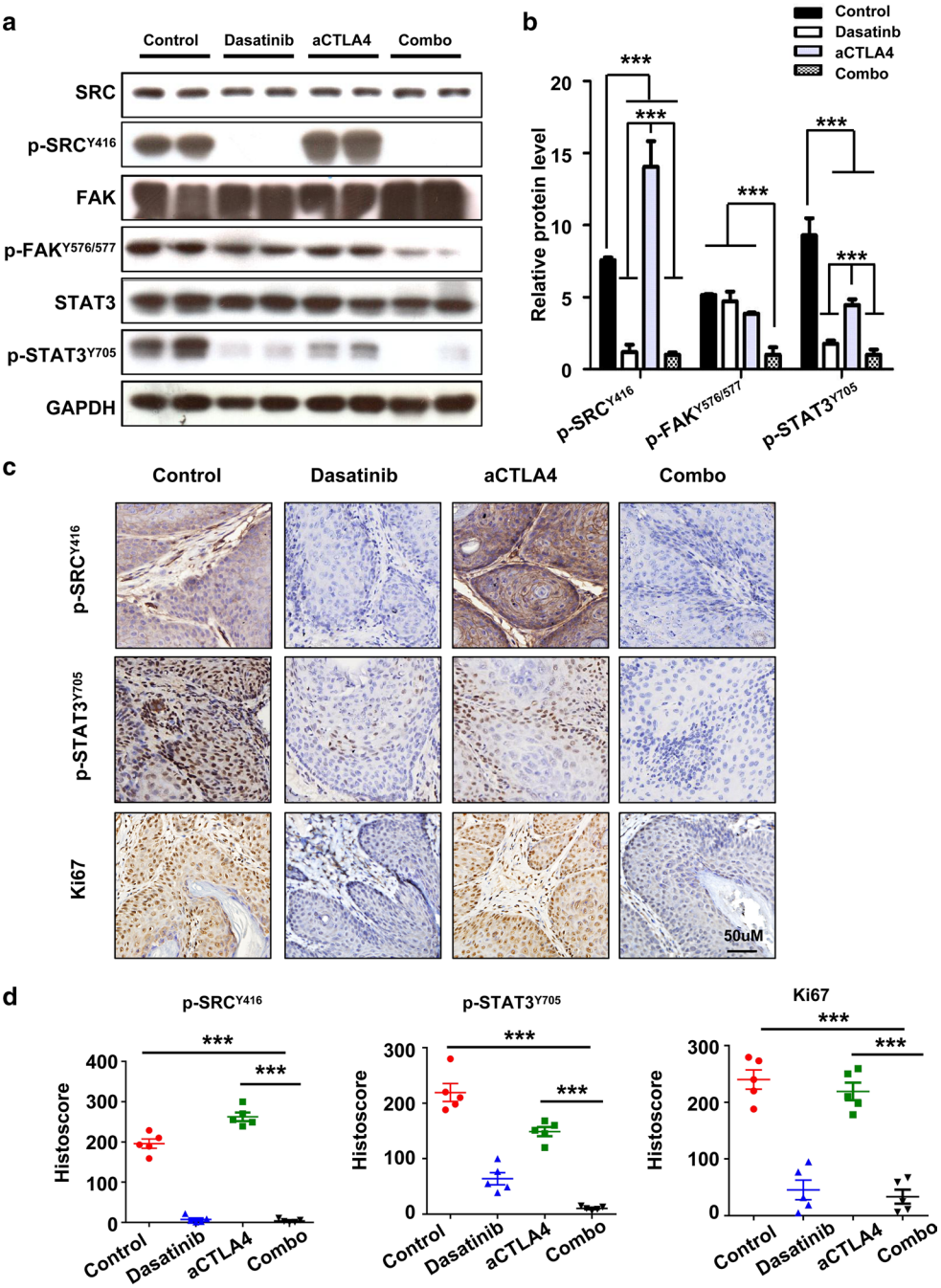

Fig. 6 Combination dasatinib with anti-mice CTLA4 therapy effectively decreased SRC family protein levels and inhibited STAT3 signalling pathway activation in *Tgfbr1/Pten* 2cKO HNSCC mouse model. **a** Western blot analysis of SRC family proteins: SRC, p-SRC^{Y416}, FAK, p-FAK$^{Y576/577}$, STAT3, and p-STAT3^{Y705} in the tumor of mice treated with PBS, alone anti-mice CTLA4 mAb, alone dasatinib, or combination treatment. GAPDH was used as the loading control. **b** Quantification of the relative protein levels for SRC, p-SRC^{Y416}, FAK, p-FAK$^{Y576/577}$, STAT3, and p-STAT3Y^{705} in each group (the data are represented as mean ± SD; ***$p < 0.001$). **c** Representative tumor immunohistochemistry images from each group for p-SRC^{Y416}, p-STAT3^{Y705}, and Ki67. Scale bar 50 µm. **d** Quantification of p-SRC^{Y416}, p-STAT3^{Y705}, and Ki67 staining in tumor from PBS, alone anti-CTLA4 mAb, alone dasatinib, or combination treatment groups. The data are represented as mean ± SD, $n = 5$ (***$p < 0.001$)

Discussion

Here, we report that the activation of SRC family protein can probably limit anti-CTLA4 chemotherapeutic efficacy in *Tgfbr1/Pten* 2cKO mice. Using this model, we found that combinational treatment with SRC inhibitor and anti-CTLA4 monoclonal antibody could effectively inhibit tumor growth in *Tgfbr1/Pten* 2cKO mice. Dasatinib effectively blocked the activation of SRC family proteins. We observed the increase in p-SRC^{Y416} protein level after anti-CTLA4 chemotherapeutic treatment, and this effect was prevented by dasatinib. In addition, we were surprised to observe the down-regulation of p-STAT3^{Y706} protein level. Cell population analysis suggested combining anti-CTLA4 and dasatinib treatment enhanced anti-tumor immunity by decreasing the number of MDSCs and Tregs, and increasing $CD4^+$ and $CD8^+$ T cells in the tumor microenvironment. Meanwhile, the combination of anti-CTLA4 and dasatinib improved the IFN-γ secretion of $CD8^+$ T cells.

CTLA4 is primarily expressed on the surface of T cells and plays a negative role in T-cell activation [16]. Inhibiting CTLA4 using anti-CTLA4 monoclonal antibody is a promising therapeutic strategy for improving the anti-tumor immune response. Up to now, several anti-CTLA4 monoclonal antibodies have been approved to treat certain malignant tumors, such as melanoma, prostate cancer, and non-small-cell lung cancer [17–19]. Unfortunately, the patient response rate for CTLA4 inhibitors in clinical practice is not very high. For example, approximately only 20% of patients with metastatic melanoma who accepted ipilimumab treatment have a greater than 5-year survival time [20]. Therefore, the mechanism of resistance to cancer immunotherapy is an urgent problem that requires a solution to improve clinical outcomes. On-going studies suggest that both tumor cell intrinsic and extrinsic factors contribute to the resistance of cancer immunotherapy. Tumor cell intrinsic factors that inhibit the anti-tumor immune response include over-expression or down-regulation of certain genes and signalling pathways in tumor cells [21]. A number of tumor cell intrinsic mechanisms have recently been confirmed, such as activation of the PI3K signalling pathway and down-regulation of the IFN-γ signalling pathway [22, 23]. In the current study, we observed the over-activation of SFKs after anti-CTLA4 chemotherapy in our HNSCC mouse model. SFKs can promote tumor cell survival and invasion, and can exert a profound effect on the tumor immune microenvironment [24, 25]. Dasatinib is a small molecule tyrosine kinase inhibitor that exerts a dual inhibition on BCR–ABL and SFKs signalling [11]. Dasatinib has been reported to inhibit tumor cell duplication and to promote tumor cell death in multiple cancer types [26, 27]. Our work and other study have consistently found that dasatinib significantly inhibits tumor growth in HNSCC in vitro and in vivo [28, 29]. These results indicate that the activation of SFKs may be a mechanism for anti-CTLA4 immunotherapy resistance. Interestingly, anti-CTLA4 treatment showed different effects on SFKs signalling in prophylactic setting and chemotherapeutic setting. According to recent in vivo studies, it has shown that SFKs may have the possibility to regulate tumor progression more than to initiate neoplasia [30–32]. These may indicate that anti-CTLA4 treatment may effectively inhibit tumor initiation in the prophylactic setting, which lead to the inhibitory effects on SFKs pathway. However, in the chemotherapeutic treatment, anti-CTLA4 mAb was administrated after tumor initiation as well as the activation of SFKs. Under these circumstances, the molecular interaction network is complex. It remains further investigations to explain the potential mechanisms.

Meanwhile, MDSCs, Tregs, and other immune suppressive cells, which can act as tumor cell extrinsic factors, play another considerable role in cancer immunotherapy resistance [33]. In our tumor-bearing mice, we found that a significant number of MDSCs and Tregs infiltrate in the tumor microenvironment [14, 34]. A number of studies have shown that the depletion of MDSCs or Tregs from the tumor microenvironment can improve or rescue anti-tumor immunity [35, 36]. However, after anti-CTLA4 chemotherapeutic treatment, the number of Tregs was not dramatically reduced in our HNSCC mice model, and nor did tumor size decrease. The existing research shows that the result of anti-CTLA4 therapy was shown to increase the ratio of $CD8^+$ T cells to Tregs [37]. If immunotherapy is unable to increase this ratio, the tumor is likely to be resistant to treatment. In the current study, single anti-CTLA4 treatment alone was insufficient to increase the ratio of $CD8^+$ T cells to Tregs in our mouse model. Based on our group previous study [29], in which dasatinib was found to successfully inhibit tumor growth by reducing MDSCs and Tregs counts, we carried co-treated mice with anti-CTLA4 mAbs and dasatinib. As expected, dasatinib rescued the anti-CTLA4 immunotherapy resistance and significantly inhibited tumor growth in mice model.

Cell proliferation plays a central role in tumor survival and growth [38]. In this study, single anti-CTLA4 mAbs or dasatinib treatment did not significantly reduced the expression of Ki-67. In addition, we found that the change of p-STAT3^{Y705} expression correlated with the expression of Ki-67. The JAK/STAT3 signalling pathway regulates many tumor biological processes, such as proliferation, angiogenesis, and invasion [39]. We speculated that the expression of Ki-67 was regulated by STAT3 activation. Notably, combination therapy with anti-CTLA4 mAbs and dasatinib treatment effectively reduced the expression of p-STAT3^{Y705} and Ki-67 in our mice model.

The drug resistance of tumor is an urgent clinical problem and combination drug therapy is one of the strategies to

address this issue. Overcoming resistance to immunotherapy is currently being studied. Specifically, there are many combination treatment strategies is being tested in clinical trials, such as combination checkpoint blockade, checkpoint blockade plus immune-stimulatory agent and checkpoint blockade plus targeted therapies [21]. The elucidation of immunotherapy resistance mechanism will bring new hope for patients with malignant tumor.

In summary, we validated that a combination of anti-CTLA4 mAbs and dasatinib therapy is an efficacious therapeutic in *Tgfbr1/Pten* 2cKO mouse model. Further studies on changes in the tumor microenvironment and the mechanism of protein regulation may provide important clues for future clinical application in humans.

Acknowledgements We thank Zhi-Yong Chen and Dong Chen for excellent technical support. And also thank Wuhan Institute of Biotechnology for their Public Technology Service Platform. Meanwhile, this study was supported by National Natural Science Foundation of China (NFSC): 81672668, 81472528, and 81472529, and the Fundamental Research Funds for the Central Universities (2042017kf0171).

Compliance with ethical standards

Ethical standards Animal studies were approved and supervised by the Animal Care and Use Committee of Wuhan University. The ethical approval number is 2014C66.

Conflict of interest The authors declare that they have no competing interests.

References

1. Bose P, Brockton NT, Dort JC (2013) Head and neck cancer: from anatomy to biology. Int J Cancer 133:2013–2023
2. Siegel RL, Miller KD, Jemal A (2017) Cancer statistics, 2017. CA Cancer J Clin 67:7–30
3. Ferris RL (2015) Immunology and immunotherapy of head and neck cancer. J Clin Oncol 33:3293–3304
4. Jie HB, Schuler PJ, Lee SC, Srivastava RM, Argiris A, Ferrone S, Whiteside TL, Ferris RL (2015) CTLA-4(+) regulatory T cells increased in cetuximab-treated head and neck cancer patients suppress NK cell cytotoxicity and correlate with poor prognosis. Cancer Res 75:2200–2210
5. Weed DT, Vella JL, Reis IM, De la Fuente AC, Gomez C, Sargi Z, Nazarian R, Califano J, Borrello I, Serafini P (2015) Tadalafil reduces myeloid-derived suppressor cells and regulatory T cells and promotes tumor immunity in patients with head and neck squamous cell carcinoma. Clin Cancer Res 21:39–48
6. Moy JD, Moskovitz JM, Ferris RL (2017) Biological mechanisms of immune escape and implications for immunotherapy in head and neck squamous cell carcinoma. Eur J Cancer 76:152–166
7. Economopoulou P, Agelaki S, Perisanidis C, Giotakis EI, Psyrri A (2016) The promise of immunotherapy in head and neck squamous cell carcinoma. Ann Oncol 27:1675–1685
8. Baumeister SH, Freeman GJ, Dranoff G, Sharpe AH (2016) Coinhibitory pathways in immunotherapy for cancer. Annu Rev Immunol 34:539–573
9. Yu GT, Bu LL, Zhao YY, Mao L, Deng WW, Wu TF, Zhang WF, Sun ZJ (2016) CTLA4 blockade reduces immature myeloid cells in head and neck squamous cell carcinoma. Oncoimmunology 5:e1151594
10. Patel A, Sabbineni H, Clarke A, Somanath PR (2016) Novel roles of Src in cancer cell epithelial-to-mesenchymal transition, vascular permeability, microinvasion and metastasis. Life Sci 157:52–61
11. Montero JC, Seoane S, Ocana A, Pandiella A (2011) Inhibition of SRC family kinases and receptor tyrosine kinases by dasatinib: possible combinations in solid tumors. Clin Cancer Res 17:5546–5552
12. Baselga J, Cervantes A, Martinelli E, Chirivella I, Hoekman K, Hurwitz HI, Jodrell DI, Hamberg P, Casado E, Elvin P et al (2010) Phase I safety, pharmacokinetics, and inhibition of SRC activity study of saracatinib in patients with solid tumors. Clin Cancer Res 16:4876–4883
13. Herold CI, Chadaram V, Peterson BL, Marcom PK, Hopkins J, Kimmick GG, Favaro J, Hamilton E, Welch RA, Bacus S, Blackwell KL (2011) Phase II trial of dasatinib in patients with metastatic breast cancer using real-time pharmacodynamic tissue biomarkers of Src inhibition to escalate dosing. Clin Cancer Res 17:6061–6070
14. Bian Y, Hall B, Sun ZJ, Molinolo A, Chen W, Gutkind JS, Waes CV, Kulkarni AB (2012) Loss of TGF-beta signaling and PTEN promotes head and neck squamous cell carcinoma through cellular senescence evasion and cancer-related inflammation. Oncogene 31:3322–3332
15. Sun ZJ, Zhang L, Hall B, Bian Y, Gutkind JS, Kulkarni AB (2012) Chemopreventive and chemotherapeutic actions of mTOR inhibitor in genetically defined head and neck squamous cell carcinoma mouse model. Clin Cancer Res 18:5304–5313
16. Wolchok JD, Saenger Y (2008) The mechanism of anti-CTLA-4 activity and the negative regulation of T-cell activation. Oncologist 13(Suppl 4):2–9
17. Wen X, Ding Y, Li J, Zhao J, Peng R, Li D, Zhu B, Wang Y, Zhang X, Zhang X (2017) The experience of immune checkpoint inhibitors in Chinese patients with metastatic melanoma: a retrospective case series. Cancer Immunol Immunother 66:1153–1162
18. Cabel L, Loir E, Gravis G, Lavaud P, Massard C, Albiges L, Baciarello G, Loriot Y, Fizazi K (2017) Long-term complete remission with ipilimumab in metastatic castrate-resistant prostate cancer: case report of two patients. J Immunother Cancer 5:31
19. Bagley SJ, Kothari S, Aggarwal C, Bauml JM, Alley EW, Evans TL, Kosteva JA, Ciunci CA, Gabriel PE, Thompson JC et al (2017) Pretreatment neutrophil-to-lymphocyte ratio as a marker of outcomes in nivolumab-treated patients with advanced non-small-cell lung cancer. Lung Cancer 106:1–7
20. Schadendorf D, Hodi FS, Robert C, Weber JS, Margolin K, Hamid O, Patt D, Chen TT, Berman DM, Wolchok JD (2015) Pooled analysis of long-term survival data from phase II and phase III Trials of ipilimumab in unresectable or metastatic melanoma. J Clin Oncol 33:1889–1894
21. Sharma P, Hu-Lieskovan S, Wargo JA, Ribas A (2017) Primary, adaptive, and acquired resistance to cancer immunotherapy. Cell 168:707–723
22. Gao J, Shi LZ, Zhao H, Chen J, Xiong L, He Q, Chen T, Roszik J, Bernatchez C, Woodman SE et al (2016) Loss of IFN-gamma pathway genes in tumor cells as a mechanism of resistance to anti-CTLA-4 therapy. Cell 167(397–404):e9
23. Peng W, Chen JQ, Liu C, Malu S, Creasy C, Tetzlaff MT, Xu C, McKenzie JA, Zhang C, Liang X et al (2016) Loss of PTEN

promotes resistance to T cell-mediated immunotherapy. Cancer Discov 6:202–216
24. Guarino M (2010) Src signaling in cancer invasion. J Cell Physiol 223:14–26
25. Kreutzman A, Ilander M, Porkka K, Vakkila J, Mustjoki S (2014) Dasatinib promotes Th1-type responses in granzyme B expressing T-cells. Oncoimmunology 3:e28925
26. Okamoto W, Okamoto I, Yoshida T, Okamoto K, Takezawa K, Hatashita E, Yamada Y, Kuwata K, Arao T, Yanagihara K et al (2010) Identification of c-Src as a potential therapeutic target for gastric cancer and of MET activation as a cause of resistance to c-Src inhibition. Mol Cancer Ther 9:1188–1197
27. Nagaraj NS, Smith JJ, Revetta F, Washington MK, Merchant NB (2010) Targeted inhibition of SRC kinase signaling attenuates pancreatic tumorigenesis. Mol Cancer Ther 9:2322–2332
28. Johnson FM, Saigal B, Talpaz M, Donato NJ (2005) Dasatinib (BMS-354825) tyrosine kinase inhibitor suppresses invasion and induces cell cycle arrest and apoptosis of head and neck squamous cell carcinoma and non-small cell lung cancer cells. Clin Cancer Res 11:6924–6932
29. Mao L, Deng WW, Yu GT, Bu LL, Liu JF, Ma SR, Wu L, Kulkarni AB, Zhang WF, Sun ZJ (2017) Inhibition of SRC family kinases reduces myeloid-derived suppressor cells in head and neck cancer. Int J Cancer 140:1173–1185
30. Kim LC, Song L, Haura EB (2009) Src kinases as therapeutic targets for cancer. Nat Rev Clin Oncol 6:587–595
31. Verhagen AM, Wallace ME, Goradia A, Jones SA, Croom HA, Metcalf D, Collinge JE, Maxwell MJ, Hibbs ML, Alexander WS et al (2009) A kinase-dead allele of Lyn attenuates autoimmune disease normally associated with Lyn deficiency. J Immunol 182:2020–2029
32. Hochgrafe F, Zhang L, O'Toole SA, Browne BC, Pinese M, Porta Cubas A, Lehrbach GM, Croucher DR, Rickwood D, Boulghourjian A et al (2010) Tyrosine phosphorylation profiling reveals the signaling network characteristics of Basal breast cancer cells. Cancer Res 70:9391–9401
33. Maccalli C, Parmiani G, Ferrone S (2017) Immunomodulating and immunoresistance properties of cancer-initiating cells: implications for the clinical success of immunotherapy. Immunol Investig 46:221–238
34. Yu GT, Bu LL, Huang CF, Zhang WF, Chen WJ, Gutkind JS, Kulkarni AB, Sun ZJ (2015) PD-1 blockade attenuates immunosuppressive myeloid cells due to inhibition of CD47/SIRPalpha axis in HPV negative head and neck squamous cell carcinoma. Oncotarget 6:42067–42080
35. Linehan DC, Goedegebuure PS (2005) $CD25^{+}CD4^{+}$ regulatory T-cells in cancer. Immunol Res 32:155–168
36. Qian L, Liu Y, Wang S, Gong W, Jia X, Liu L, Ye F, Ding J, Xu Y, Fu Y, Tian F (2017) NKG2D ligand RAE1epsilon induces generation and enhances the inhibitor function of myeloid-derived suppressor cells in mice. J Cell Mol Med 21:2046–2054
37. Quezada SA, Peggs KS, Curran MA, Allison JP (2006) CTLA4 blockade and GM-CSF combination immunotherapy alters the intratumor balance of effector and regulatory T cells. J Clin Investig 116:1935–1945
38. Boroughs LK, DeBerardinis RJ (2015) Metabolic pathways promoting cancer cell survival and growth. Nat Cell Biol 17:351–359
39. Banerjee K, Resat H (2016) Constitutive activation of STAT3 in breast cancer cells: a review. Int J Cancer 138:2570–2578